Photoinduced interlayer diffusion in *a*-Ge/Se multilayers

M. W. Wright* and H. J. Trodahl
Department of Physics, Victoria University of Wellington, Private Bag, Wellington, New Zealand
(Received 2 February 1987)

We have studied photoinduced interlayer diffusion in *a*-Ge/Se multilayers by monitoring changes in the Raman spectra under the laser illumination required by the Raman measurement. We present a model that reproduces most of the observed changes to the Raman spectrum, and have been able to extract values for the photoinduced diffusion cross section for four of the intense Kr^+ laser lines.

I. INTRODUCTION

Photoinduced changes in the properties of chalcogenide glasses are well-documented phenomena, which have been reviewed in a recent paper by Elliot.[1] Amorphous Ge_xSe_{1-x} in particular displays photoinduced diffusion,[2] and we have recently demonstrated that Raman measurements on deliberately layered a-Ge/Se samples can yield a diffusion cross section in this material.[3] The measurement relies on an estimate, using their Raman signatures, of the relative densities of $GeSe_4$ and Se_2 units (see Fig. 1) within the Raman-probed region. As the Ge and Se layers mix under strong laser illumination the $GeSe_4$ density grows at the expense of Se—Se bonds, and the planar symmetry of layered samples permits extraction of the diffusion rate. Our preliminary work[3] was limited to a study under only one line (5309 Å) of a Kr^+ laser, and relied on a rather crude analysis. In the present paper we refine the analysis and extend the measurements to the rest of the visible region.

We start our discussion in the next section with a model of the diffusion process and the Raman measurement. The diffusion process will be followed past the point at which the layers near the surface mix completely, and the subsequent reaction front profile and advance will be modeled.

In Sec. III we describe the production of the multilayer Ge/Se samples and their characterization. The Raman measurements are also described briefly. The results and their comparison with the model are given in Sec. IV.

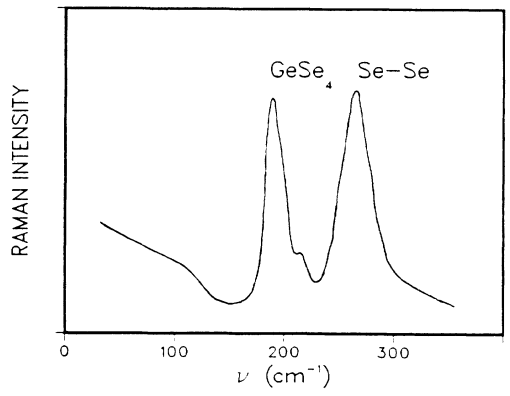

FIG. 1. Typical Raman spectra of mixed *a*-Ge_x Se_{1-x}. The structural units responsible for the two prominent features are identified.

II. PHOTOINDUCED DIFFUSION IN THE MULTILAYERS

Raman spectra of Ge/Se multilayers show a change, under illumination, of the 197- and 265-cm^{-1} lines associated with the $GeSe_4$ and Se_2 units. These changes signal the growth of a mixed layer at the Ge/Se interfaces, and are related to the following structural changes: (i) the $GeSe_4$ density grows at the expense of Se_2 density. (ii) the homopolar bonds Se—Se and Ge—Ge are replaced by heteropolar bonds Ge—Se, rendering the material more transparent.[4] As a result of (ii) the laser intensity at depth increases with time, and it is this that ultimately controls the advance of a reaction front through the material.

Modeling of this process is simplified by noting that of the two length scales in the problem, the skin depth δ is much larger than the modulation period p. As a consequence the illumination can be treated as uniform through any single partially mixed interfacial layer. We therefore discuss this problem first.

A. Growth of a single interfacial layer

There is considerable evidence that the photoinduced diffusion in amorphous chalcogenides proceeds by the rearrangement of the homopolar chalcogen bonds,[2] and we build this feature into our model from the outset. Thus diffusion takes place only in regions where Se—Se bonds exist, i.e., in regions where the local Ge composition x (Ge_xSe_{1-x}) is less than $\frac{1}{3}$. A mixed layer then grows by the diffusion of Se atoms from a pure Se region at $y<0$, through a Se rich layer to an interface between $GeSe_2$ and pure Ge at $y=a$ (see Fig. 2). The composition across the mixed layer is determined by applying Fick's law,

$$\frac{dn}{dt} = -D\frac{\partial \rho_e}{\partial y} ,$$

where dn/dt is the flux of Se atoms and ρ_e is the density of Se atoms in excess of $GeSe_2$ (equal to the density of Se—Se bonds). D is the diffusion coefficient, given in terms of

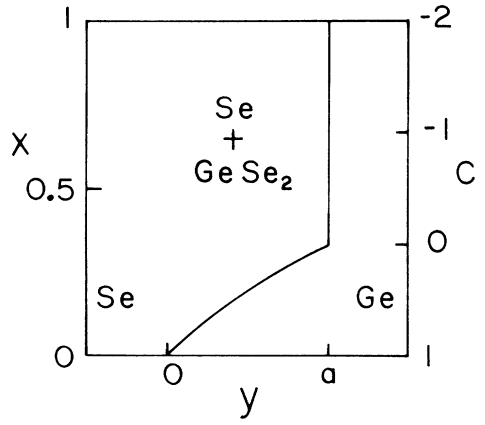

FIG. 2. Schematic composition profile through the mixed layer lying between pure a-Se ($y<0$) and pure a-Ge ($y>a$).

the step frequency f and length l as

$$D=\frac{l^2}{6}f=\frac{l^2}{6}\frac{\sigma F}{h\nu} . \tag{1}$$

Here F is the radiation flux (power to area) in the interfacial layer, $h\nu$ is the photon energy, and σ the diffusion cross section.

The Se flux feeds the growth of the mixed layer, and is related to the Se-atom density $\rho_{Se}(y,t)$ by

$$\frac{dn}{dt}=\frac{\partial}{\partial t}\int_y^a \rho_{Se}dy .$$

Note that ρ_e and ρ_{Se} are not the same density, for the latter includes those Se atoms locked by two Ge—Se bonds. For this reason it is convenient to write the above equations in terms of the total (Ge plus Se) atomic density ρ_0 and the concentration $[c(y,t)]$ of excess Se atoms, defined by

$$Ge_xSe_{1-x}=cSe+(1-c)Ge_{1/3}Se_{2/3} .$$

In these variables

$$\rho_{Se}=(1-x)\rho_0=\tfrac{1}{3}(c+2)\rho_0 ,$$

$$\rho_e=c\rho_0 .$$

In the absence of any firm information about the composition dependence of the atomic density of a-Ge_xSe_{1-x} we have set it equal to a constant (ρ_0), independent of x. Within this approximation the above equations become

$$\frac{\partial}{\partial t}\int_y^a (2+c)dy=-3D\frac{\partial c}{\partial t} ,$$

with the conditions

$$c(0)=1 ,$$

$$c(a)=0 .$$

The solution is straightforward, resulting in

$$c(y)=-\mathrm{erf}(ky/a)/\mathrm{erf}(k) , \tag{2}$$

where

$$k=0.4325...$$

and

$$\frac{da^2}{dt}=\beta D,\quad \beta=2.592.... \tag{3}$$

The average density of $GeSe_4$ units in the mixed layer is given by an integral of $1-c$ through the layer,

$$\rho_t\int_0^a (1-c)dy/a=\alpha\rho_t ,$$
$$\alpha=0.518... , \tag{4}$$

where ρ_t ($=\rho_0/3$) is the density of $GeSe_4$ tetrahedral units in a-$GeSe_2$.

The function of Eq. (2) is plotted in Fig. 3, and it can be seen to approximate quite closely the linear profile assumed in our earlier report.[3] The similarity is a result of the fact that 80% of the Se atoms entering the mixed layer are required to form the alloy $GeSe_2$ at the $GeSe_2$/Ge interface; only 20% fill the excess Se requirements through the bulk of the mixed layer. The Se flux, and thus the slope dc/dy, varies by only 20% across the layer. The linear composition profile gave a coefficient of 3 in Eq. (3). The resulting error was partially compensated by the use of the factor 0.5 in place of the 0.518 of Eq. (4) when estimating the mixed layer thickness from Raman spectra. Consequently the linear approximation led to a small (7%) but systematic overestimate of the diffusion cross section σ.

B. Advance of the reaction

We now set up the equations governing the advance of the reaction front into the multilayer film. We characterize the material at depth z and time t by the average over one modulation period of the $GeSe_4$ (tetrahedron) and Se_2 (dimer) densities, $n_t(z,t)$ and $n_d(z,t)$, given throughout in units of the total atomic density ρ_0. In the absence of

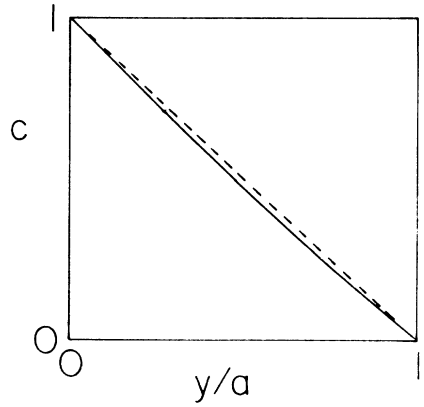

FIG. 3. Fick's-law solution for the excess Se composition (c) profile across the mixed-layer region. The dashed line is the linear profile assumed in an earlier publication.

mixing across the Ge/Se interfaces there would be only pure Ge and pure Se layers, and

$$n_t(z,0)=0 \qquad (5)$$
$$n_d(z,0)=d_{\mathrm{Se}}/p \ ,$$

where d_{Se} is the initial Se layer thickness. (Note that in the twofold-coordinated Se network there is one Se_2 unit for each Se atom.) Upon the formation of mixed layers, each $GeSe_4$ unit forms at the expense of two Se—Se bonds, so that

$$n_d(z,t)=d_{\mathrm{Se}}/p-2n_t(z,t) \ . \qquad (6)$$

Our samples were prepared on the Se-rich side of $GeSe_2$, so that the reaction ceased when the Ge layer was depleted. This occurs when each Ge atom is locked into a $GeSe_4$ unit, i.e., when

$$n_t(\text{saturation})=d_{\mathrm{Ge}}/p=1-d_{\mathrm{Se}}/p \ , \qquad (7)$$

where d_{Ge} $(=p-d_{\mathrm{Se}})$ is the initial Ge-layer thickness.

Following Eq. (4), the average density n_t is given in terms of the mixed layer thickness a and period p, as

$$n_t=\frac{2\rho_t}{\rho_0}\alpha a/p=\frac{2\alpha}{3}a/p \ , \qquad (8)$$

where the factor of 2 results from the two Ge/Se interfaces on each Ge layer. The rate of growth of n_t is then given by

$$\frac{d(n_t^2)}{dt}=\frac{4\alpha^2\beta}{9p^2}\frac{l^2\sigma}{6h\nu}F(z,t) \ . \qquad (9)$$

The flux at depth z is related to the incident flux F_0 by

$$F(z,t)=F_0(1-R)\exp\left[-\int_0^z \eta(z,t)dz\right] , \qquad (10)$$

where R is the surface reflectivity and η is the absorption coefficient. η carries contributions from all three bond types, but our work has been carried out at photon energies for which Ge—Ge bonds form the strongest absorption.[4] We therefore take the absorption coefficient to be that contributed by the volume fraction of *a*-Ge remaining at (z,t), i.e.,

$$\eta(z,t)=\eta_{\mathrm{Ge}}\left[d_{\mathrm{Ge}}/p-n_t(z,t)\right] . \qquad (11)$$

Equations (5–11) are sufficient to determine the advance of the reaction. They are first conveniently rewritten in terms of reduced dimensionless coordinates for time,

$$\tau=\left[\frac{4\alpha^2\beta}{9d_{\mathrm{Ge}}^2}\frac{l^2\sigma}{6h\nu}F_0(1-R)\right]t \ , \qquad (12)$$

depth,

$$\zeta=\left[\eta_{\mathrm{Ge}}d_{\mathrm{Ge}}/p\right]z \ , \qquad (13)$$

and average $GeSe_4$ tetrahedra density,

$$w(\zeta,\tau)=(p/d_{\mathrm{Ge}})n_t \ . \qquad (14)$$

In these coordinates, the reaction proceeds according to

$$\frac{d(w^2)}{dt}=\exp\left[-\int_0^{\zeta}(1-w)d\zeta\right] , \qquad (15)$$

subject to the conditions

$$w(\zeta,0)=0$$

and

$$w(\zeta,\tau)\le 1 \ .$$

The solution is again straightforward, with

$$w(\zeta,\tau)=\begin{cases}\dfrac{3}{2+\exp[\zeta-\zeta_c(\tau)]/2}, & \zeta\ge\zeta_c \\ 1, & \zeta\le\zeta_c \ ,\end{cases} \qquad (16)$$

where

$$\zeta_c(\tau)=\begin{cases}2\ln[\tau^{1/2}/(3-2\tau^{1/2})], & \tau\le 1 \\ 3(\tau-1), & \tau>1 \ .\end{cases} \qquad (17)$$

The value $\zeta_c(\tau)$ corresponds to the depth at which the reaction is complete $(w=1)$; note that ζ_c reaches the front surface $(\zeta=0)$ when $\tau=1$ and thereafter it advances into the sample at the rate

$$\frac{d\zeta_c}{d\tau}=3 \ .$$

This advance is illustrated in Fig. 4.

The Raman estimate of the $GeSe_4$- and Se_2-unit densities are

$$\langle n_t\rangle=\int_0^{\infty}dz\, n_t\exp\left[-2\int_0^z\eta dz\right] , \qquad (18a)$$
$$\langle n_d\rangle=\int_0^{\infty}dz\, n_d\exp\left[-2\int_0^z\eta dz\right] . \qquad (18b)$$

It is only the ratio of line strengths that is easily measured;

$$r\equiv\frac{\langle n_t\rangle}{\langle n_d\rangle}=\frac{d_{\mathrm{Ge}}\langle w\rangle}{d_{\mathrm{Se}}-2d_{\mathrm{Ge}}\langle w\rangle} \ , \qquad (19)$$

where

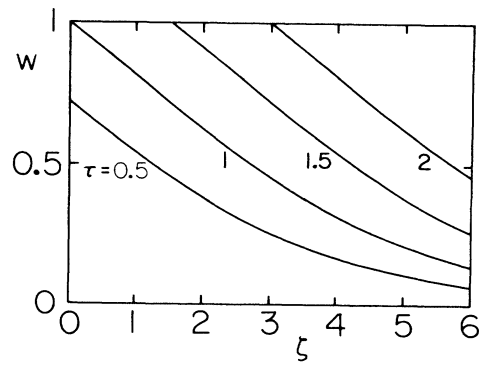

FIG. 4. Plots, in reduced coordinates, of the $GeSe_4$ unit density w vs depth ζ for four different times τ. The advance of the reaction front is clearly seen.

$$\langle w \rangle = \frac{\int_0^\infty w\, d\xi \exp\left[-2\int_0^\xi (1-w)d\xi\right]}{\int_0^\infty d\xi \exp\left[-2\int_0^\xi (1-w)d\xi\right]} . \quad (20)$$

The evaluation of these integrals, using the solutions of Eqs. (16) and (17), leads to

$$\langle w \rangle = \begin{cases} \frac{4}{5}\tau^{1/2}\frac{45-25\tau^{1/2}}{45-24\tau^{1/2}}, & \tau \le 1 \\ \frac{30\tau-14}{30\tau-9}, & \tau \ge 1 . \end{cases} \quad (21)$$

In Fig. 5 we show a plot of $\langle w \rangle^2$ versus τ. Note that the initial rise is followed by saturation which sets in after $\tau = 1$.

An experimental estimate of $\langle w \rangle$ can be made through the measurable ratio r,

$$\langle w \rangle = \left[d_{Se}/d_{Ge}\right]\frac{r}{1+2r} , \quad (22)$$

which permits the determination of the diffusion cross section through Eqs. (12) and (21). It is also worth noting that a plot of

$$A^2 \equiv \left[d_{Se}\frac{r}{1+2r}\right]^2 \quad (23)$$

versus $F_0 t$ is predicted to yield a straight line of slope

$$\frac{4\alpha^2\beta}{9}\frac{l^2\sigma}{6h\nu}(1-R) \quad (24)$$

until the Ge layers near the surface are depleted, and thereafter begins to saturate at d_{Ge}^2. Below we use such plots to compare data taken with several samples of differing layer thicknesses.

III. EXPERIMENTAL DETAILS

The samples were prepared by evaporating Ge and Se from separate sources in a vacuum chamber with a base pressure of less than 10^{-7} torr. The rates were independently monitored and controlled to deposit Ge (Se) at 4 Å s^{-1} (13 Å s^{-1}) to a total film thickness of between 0.65 and 0.9 μm. Multilayers were formed by alternately obscuring the sources with an oscillating shutter. The total deposited thicknesses of each component were measured directly on each sample, and were combined with the shutter frequency and evaporation time to determine the average layer thicknesses d_{Ge} and d_{Se}. X-ray-interference, optical, and far-infrared data have established that the films had a well-defined multilayer structure.[3]

Raman measurements were performed in the psuedo-back-reflection geometry on samples that were rotated under the line-focused laser light. The Raman spectra developed under the exciting radiation, and we collected spectra until the changes showed signs of saturation. The area of the irradiated annulus was easily identified and measured at the completion of a Raman experiment and the result was combined with a power meter measurement to yield the average flux. Flux levels were typically 10 mW mm^{-2}, at least two orders of magnitude smaller than the flux required to cause crystalization.[5]

The ratio of the 197 and 250 cm^{-1} Raman cross sections was determined by performing Raman measurements, at each Kr^+ laser line, on a mixed sample of a-Ge Se_4. The ratio n_l/n_d in this sample is 0.5[6].

Throughout the analysis we have made the assumption that the Raman cross sections of the $GeSe_4$ and Se_2 quasi-molecular units are independent of the environment, so that Raman line strengths are proportional to the unit densities. There is considerable evidence to support this view,[6,7] based primarily on the line-strength variations with composition in a $Ge_x\ Se_{1-x}$, and on the relative insensitivity to x of line positions and widths. Note however, that there is a *weak* environment effect in the *frequency* of the $GeSe_4$ line, which shifts with composition in mixed samples.[8]

IV. RESULTS

We start this section by displaying in Fig. 6 a measurement of $\langle w \rangle^2$ versus energy dose $F_0 t$. These particular data were collected using a yellow laser line (2.18 eV), and on a sample with relatively thin layers (d_{Ge},d_{Se}) of 16 and 73 Å. The fit of Eq. (21) is seen to be excellent, except for a region near the origin where the diffusion rate appears depressed. This reduced diffusion was also found

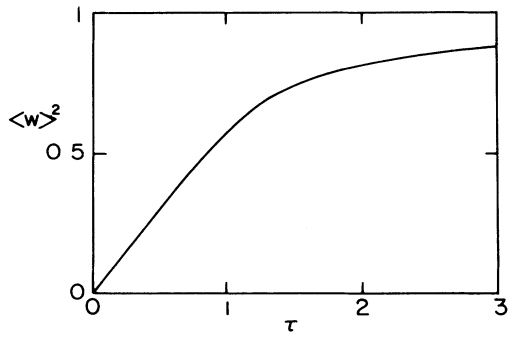

FIG. 5. Predicted variation of $\langle w \rangle^2$, the square of the Raman estimate for the $GeSe_4$ unit density, with reduced time τ. Note the approximately linear rise for $\tau < 1$.

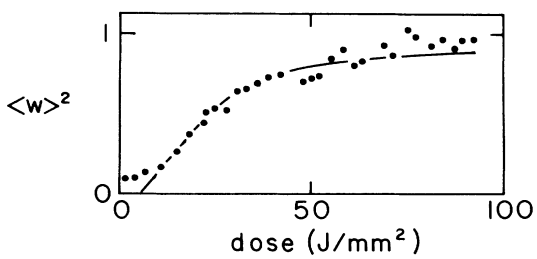

FIG. 6. A direct comparison between the Raman estimate of $\langle w \rangle^2$ [see Eq. (22)] and the growth predicted by the model. These data were taken with the 2.18-eV Kr^+ line.

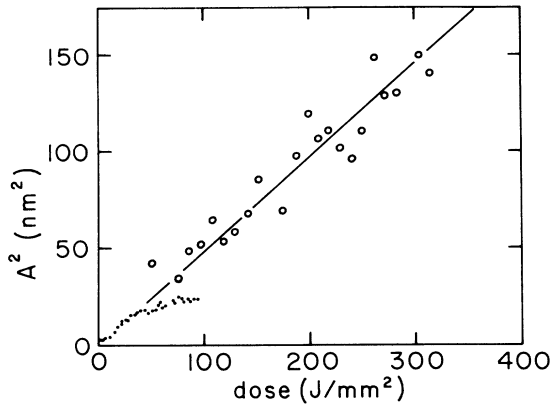

FIG. 7. A^2 vs 2.18-eV dose (F_0t) for two samples with differing d_{Ge}, d_{Se}. It can be seen that a common straight line can be used to fit the initial rises of A^2.

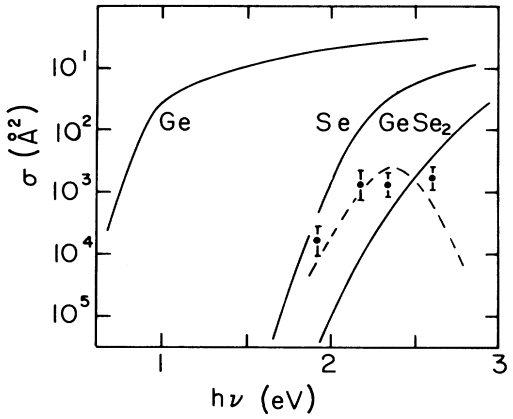

FIG. 8. Comparison of our photoinduced diffusion cross sections with the absorption cross sections per bond in a-Ge, a-Se, and a-$GeSe_2$. The photodarkening response in a-Ge_xSe_{1-x} is also shown, in arbitrary units, by the dashed line.

in our earlier work,[3] and appears to occur whenever the mixed layer thickness (a) is less than about 15 Å. The source of the reduction is unclear.

Figure 7 displays a composite (two-sample) plot of A^2 versus dose, again using the yellow (2.18-eV) line. The slope of a line drawn through the presaturation data, combined with an assumed 2.5-Å step length, yields a diffusion cross section of 2×10^{-3} Å^2. Similar measurements have been made using intense Kr^+ laser lines throughout the visible region, with at least two samples studied under each exciting line. The measured diffusion cross sections are shown plotted versus photon energy in Fig. 8. Also shown in Fig. 8 are the absorption cross sections for a-Ge,[9] a-Se,[7,10] and a-Ge Se_2 (Refs. 4-7 and 11) and, in arbitrary units, the photodarkening (PD) response function of a-Se.[10] The frequency dependence that we measure approximately follows the PD response. This supports the contention that the diffusion is a response to the disturbance of the Se—Se bonds, rather than Ge—Ge (Ge—Se) bonds found in a-Ge (a-Ge Se_2), since the photodarkening phenomena appears to be a feature of chalcogen-rich alloys and not the elemental compounds.[12] The Ge atoms predominately serve to constrain the structure through which the diffusion occurs.[1]

V. CONCLUSIONS

We have demonstrated that the photoinduced changes in the Raman spectra of amorphous Ge/Se multilayers is satisfactorily described by the diffusion of excess Se through a mixed layer to form $GeSe_2$ at a pure a-Ge interface. Our mode contains only one adjustable parameter, the diffusion cross section, which can be determined from the time evolved Raman spectra. We have consequently been able to determine, in absolute units, the value of the cross section for the four intense Kr^+ laser lines in the visible region. The magnitude of the cross section and its spectral dependence are consistent with the proposal that it is excess Se that undergoes diffusion.

ACKNOWLEDGMENT

This project received supporting grants from the New Zealand University Grants Committee and the Victoria University Internal Research Committee.

*Present address: Department of Physics and Astronomy, University of New Mexico, Albuquerque, New Mexico 87131.

[1]S. R. Elliott, J. Non-Cryst. Solids **81**, 71 (1986).
[2]G. A. N. Connell, Phys. Rev. B **24**, 4560 (1981).
[3]H. J. Trodahl, M. W. Wright, and A. Bittar, Solid State Commun. **59**, 699 (1986).
[4]H. J. Trodahl and L. Viña, Phys. Rev. B **27**, 6498 (1983).
[5]E. Haro, Z. S. Xu, J.-F. Morhange, M. Balkanski, G. P. Espinosa, and J. C. Phillips, Phys. Rev. B **32**, 969 (1985).
[6]H. J. Trodahl, J. Phys. C **17**, 6027 (1984).
[7]P. Tronc, M. Bensoussan, A. Brenac, and C. Sebenne, Phys. Rev. B **8**, 5947 (1973).
[8]K. Murase and T. Fukunaga, in *Optical Effects in Amorphous Semiconductors*, AIP Conf. Proc. No. 120, edited by P. C. Taylor and S. G. Bishop (AIP, New York, 1984), p. 457.
[9]R. G. Buckley, J. Non-Cryst. Solids **37**, 231 (1980).
[10]K. Tanaka and A. Odajima, Solid State Commun. **43**, 961 (1982).
[11]T. Takahashi and Y. Harada, J. Non-Cryst. Solids **35&36**, 1041 (1980).
[12]E. Mytilineou, P. C. Taylor, and E. A. Davis, Solid State Commun. **35**, 497 (1980).